The detectability of H I 21-cm absorption in damped Lyman-α systems

S. J. Curran* and J. K. Webb

School of Physics, University of New South Wales, Sydney NSW 2052, Australia

arXiv:astro-ph/0606180v1 8 Jun 2006

ABSTRACT

In this paper we investigate the possible reasons why H I 21-cm absorption in damped Lyman-α systems (DLAs) has only been detected at low redshift: To date, no 21-cm absorption has yet been detected at $z_{\rm abs} > 2.3$ and at redshifts less than this, there is a mix of detections and non-detections in the DLAs searched. This has been attributed to the morphologies of the galaxies hosting the DLAs, where at low redshift the DLAs comprise of both large and compact galaxies, which are believed to have low and high spin temperatures, respectively. Likewise, at high redshift the DLA population is believed to consist exclusively of compact galaxies of high spin temperature (Chengalur & Kanekar 2000; Kanekar & Chengalur 2001, 2003). However, in a previous paper (Curran et al. 2005) we found that by not assuming or assigning an, often uncertain, value for the coverage of the radio continuum source by the 21-cm absorbing gas, that there is generally no difference in the spin temperature/covering factor ratio between the 21-cm detections and non-detections or between the low and high redshift samples. Furthermore, only one of the 18 non-detections has a known host morphology, thus making any link between morphology and 21-cm detectability highly speculative.

We suggest that the lack of 21-cm absorption detections at high redshift arises from the fact that these DLAs are at similar angular diameter distances to the background quasars (i.e. the distance ratios are always close to unity): Above $z_{\rm abs} \sim 1.6$ the covering factor becomes largely independent of the DLA–QSO distance, making the high redshift absorbers much less effective at covering the background continuum emission. At low redshift, small distance ratios are strongly favoured by the 21-cm detections, whereas large ratios are favoured by the non-detections. This mix of distance ratios gives the observed mix of detections and non-detections at $z_{\rm abs} \lesssim 1.6$. In addition to the predominance of large distance ratios and non-detections at high redshift, this strongly suggests that the observed distribution of 21-cm absorption in DLAs is dominated by geometric effects.

Key words: quasars: absorption lines – cosmology: observations – cosmology: early Universe – galaxies: ISM

1 INTRODUCTION

Redshifted absorption systems lying along the sight-lines to distant quasars are important probes of the early to present day Universe. In particular, damped Lyman-α absorption systems (DLAs), where $N_{\rm HI} \geqslant 2 \times 10^{20}$ cm^{-2}, are useful since they account for at least 80% of $\Omega_{\rm neutral}$ in the Universe (Prochaska, Herbert-Fort & Wolfe 2005). Since the Lyman-α transition occurs in the ultra-violet band, direct ground based observations of neutral hydrogen are restricted to redshifts of $z \gtrsim 1.7$. However, observations of the H I spin-flip transitions at $\lambda_{\rm rest} = 21$ cm can probe from $z = 0$, thereby providing a useful complement to the high redshift optical data.

Provided the 21-cm and Lyman-α absorption arise in the same cloud complexes, the column density $N_{\rm HI}$ [cm^{-2}] of the absorbing gas in a homogeneous cloud is related to the velocity integrated optical depth of the 21-cm line via

$$N_{\rm HI} = 1.823 \times 10^{18}\, T_{\rm spin} \int \tau\, dv\,. \tag{1}$$

Here $T_{\rm spin}$ [K] is the spin temperature of the gas and so in principle, armed with the neutral hydrogen column density from an observation of the Lyman-α line, this quantity may be derived from the optical depth of the 21-cm absorption. However, the observed optical depth of the 21-cm line also depends upon on how effectively the background radio continuum is covered by the absorber via, $\tau \equiv -\ln\left(1 - \frac{\sigma}{f\,S}\right)$, where σ/S is the depth of the line relative to the flux density and f is the covering factor of the flux by the absorber.

* E-mail: sjc@phys.unsw.edu.au

In the optically thin regime ($\sigma/f.S \lesssim 0.3$), which applies to all but one of the known 21-cm absorbing DLAs[1], Equation 1 reduces to $N_{HI} = 1.823 \times 10^{18} \frac{T_{spin}}{f} \int \frac{\sigma}{S} dv$, thus giving a direct measure of the spin temperature of the gas for a known column density (from the Lyman-α line) and covering factor. However, in the absence of any direct measurement of the size of the radio absorbing region, this latter value is often assumed or at best estimated from the size of the background emission region.

From the literature, 16 of the 35 DLAs searched have been found to exhibit 21-cm absorption (see Table 1)[2], all of which occur at redshifts below $z_{abs} \leqslant 2.04$, although there are a near equal number of non-detections also below this redshift. Chengalur & Kanekar (2000); Kanekar & Chengalur (2001, 2003) therefore advocate a scenario where low redshift DLAs have a mix of low (21-cm detections) and high (21-cm non-detections) spin temperatures, with the high redshift absorbers having exclusively high spin temperatures.

However, in a previous paper (Curran et al. 2005), we find evidence that the importance of the covering factor is underestimated and the common practice of setting $f = 1$ could possibly have the effect of assigning artificially high spin temperatures to DLAs, particularly those not detected in 21-cm. Furthermore, we found no statistical difference in the spin temperature/covering factor ratio between the low and high redshift samples, although the larger absorbing galaxies (spirals) group together at low values of T_{spin}/f and z_{abs}. Since the ratio of spin temperature/covering factor is $T_{spin}/f \propto N_{HI}/\int \frac{\sigma}{S} dv$ (Equation 1), we have taken into account the total H I column density of the absorber and integrated optical depth of the 21-cm absorption (incorporating the radio flux). This suggests that the difference between the detections and non-detections is due to some other effect, a possibility which we investigate in this paper.

2   SELECTION EFFECTS

2.1   Differences between the 21-cm absorbing and non-absorbing DLAs

We note that the cut-off of the 21-cm detections, $z_{abs} = 2.04$, is close to the atmospheric cut-off of the Lyman band at $z_{abs} = 1.7$ and over the range from which the Mg II 2796/2803 Å doublet may be observed by ground-based telescopes ($0.2 \leqslant z_{abs} \leqslant 2.2$). Indeed only 4 of the 17 H I 21-cm detections occur in DLAs originally identified through the Lyman-α line, cf. 13 of the 18 non-detections. Mg II selection gives rise to a range of absorbing galaxy types (Churchill, Kacprzak & Steidel 2005), and although most DLAs discovered through the Lyman-α line have unidentified host types (mainly due to the high redshift selection, e.g. Table 1), low redshift studies suggest that equal numbers of dwarfs and spirals should contribute to the DLA population (Ryan-Weber, Webster & Staveley-Smith 2003; Zwaan et al. 2005). In Table 1 we see that the DLAs detected in 21-cm absorption exhibit a variety of host galaxy types, although there is the strong preference for 21-cm absorption to occur in Mg II selected sources. However, Curran, Webb & Murphy (2006) find that, while the 21-cm line strength appears correlated to the rest frame
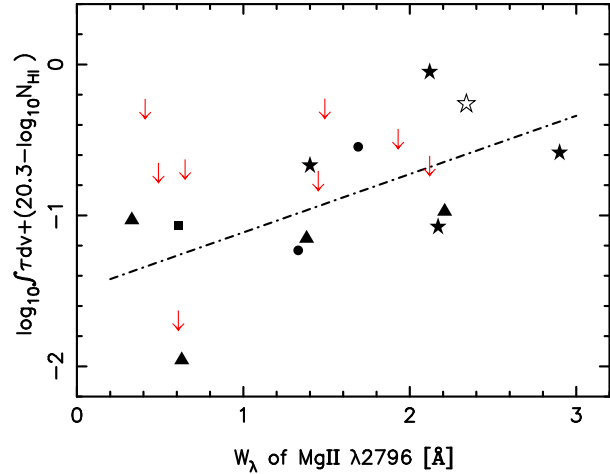

Figure 1. The normalised velocity integrated optical depth ($\int \tau \, dv/N_{HI} \propto f/T_{spin}$) versus the rest frame equivalent width of the Mg II 2796 Å line. The shapes (explained in Fig. 2) represent the 21-cm detections and the arrows show the upper limits for the non-detections. The line shows the least-squares fit for the 21-cm detections. Adapted from Curran, Webb & Murphy (2006).

equivalent width of the Mg II line, 21-cm absorption is perfectly detectable at low equivalent widths. Furthermore, large equivalent widths do not necessarily ensure a detection of 21-cm absorption (Fig. 1).

Since host type and Mg II equivalent width seem incidental in determining whether 21-cm absorption is detected, we suggest that the spin temperature/covering factor ratios in the DLAs searched for in 21-cm absorption are due to geometric effects introduced by the DLA discovery method: In Fig. 2 we show the spin temperature/covering factor ratio against the ratio of the angular diameter distances[3] to the absorber and background continuum. Although the sizes and morphologies of the radio sources differ considerably (Table 2 of Curran et al. 2005), for given background continuum size and 21-cm absorbing cross section, the covering factor is obviously larger for those absorbers, at least at low redshift (Fig. 3), which are located very much closer to us than the radio emitter. Indeed we see that the DLAs not detected in 21-cm have significantly larger angular diameter distance ratios than the detections, with the vast majority of these having ratios of $DA_{DLA}/DA_{QSO} \gtrsim 0.9$ (Fig. 2)[4].

In order to demonstrate the differences in fractional distances between the 21-cm detections and non-detections, in Fig. 3 we show how the distance ratio is distributed with absorber redshift. We see that most of the 21-cm detections are located in the bottom left quadrant, defined here by $DA_{DLA}/DA_{QSO} \leqslant 0.8$ and $z_{abs} \leqslant 1.6$. This is the approximate redshift of the turnover in the angular diameter distance, where objects increase their angular

---

[1] 0235+164 (Roberts et al. 1976).

[2] Since radio frequency interference (RFI) prevented reliable observations of 0432–440 and 1228–113 (Curran et al. 2005), these are not included in the analysis.

[3] See Peacock (1999); Hogg (1999).

[4] We note that two 21-cm absorbers which are associated with LSBs, which we expect to provide relatively small coverage, are located at a fractional distance of $\gtrsim 0.9$. These are 1157+014 (ratio = 1.00) and 1328+307 (ratio = 0.93). At $z_{abs} = 1.94$, the former is one of the highest redshifted 21-cm absorbers known and occults a radio source size of < 1.2 arc-secs (Stocke et al. 1984) and 1328+307 occults a core dominated source of 2.57 arc-secs (van Breugel et al. 1992). Despite the pitfalls in assuming given absorber and emitter sizes, for the larger number of non-detections, the distribution does appear very skewed towards high fractional distances.

Table 1. DLAs and sub-DLAs searched for 21-cm absorption. As per Curran et al. (2005), in the top panel we list the detections and in the bottom panel the non-detections. $z_{\rm abs}$ and $N_{\rm HI}$ are the redshift and total neutral hydrogen column density [cm^{-2}] of the DLA, respectively, with the optical identification (ID) given: D–dwarf, L–LSB, S–spiral, U–unknown. The transition through which the DLA was originally identified is given. Finally we give the quasar redshift and corresponding angular diameter distance for between the quasar and absorber (Hogg 1999) [throughout this paper we use $H_0 = 75$ km s^{-1} Mpc^{-1}, $\Omega_{\rm matter} = 0.27$ and $\Omega_\Lambda = 0.73$].

QSO	$z_{\rm abs}$	$\log N_{\rm HI}$	ID	Transition	Ref	$z_{\rm em}$	$D_{\rm A12}$ [Mpc]
0235+164	0.52385	21.7	S	Mg II	1	0.940	588
0248+430	0.394	–	U	Mg II	2	1.31	1026
0438–436[†]	2.347	20.8	U	Ly-α	20	2.852	144
0458–020	2.03945	21.7	U	Ly-α	3	2.286	98
0738+313	0.2212	20.9	D	Mg II	4	0.635	822
...	0.0912	21.2	U	Ly-α	5	...	1119
0809+483[a]	0.4369	20.3	S	21-cm	6	0.871	665
0827+243	0.5247	20.3	S	Mg II	7	0.939	584
0952+179	0.2378	21.3	L	Mg II	2	1.472	1301
1127–145	0.3127	21.7	L	Mg II	8	1.187	1093
1157+014	1.94362	21.8	L	Ly-α	9	1.986	20
1229–021	0.39498	20.8	S	Mg II	10	1.045	882
1243–072	0.4367	–	S	Mg II	11,12	1.286	955
1328+307[b]	0.692154	21.3	L	21-cm	13	0.849	227
1331+170	1.77642	21.2	U	Si IV	14	2.084	146
1629+120	0.5318	20.7	S	Mg II	15	1.795	995
2351+456	0.779452	–	U	21-cm	16	1.9864	790
0118–272	0.5579	20.3	U	Mg II	17	0.559	2
0201+113	3.386	21.4	U	Ly-α	18	3.610	43
0215+015	1.3439	19.9	U	Ly-α	19	1.715	242
0335–122	3.178	20.8	U	Ly-α	20	3.442	50
0336–017	3.0619	21.2	U	Ly-α	21	3.197	29
0439–433	0.10097	~ 20.0	U	Mg II	22	0.593	1048
0454+039	0.8596	20.7	D	Mg II	23	1.345	461
0528–250	2.811	21.3	U	Ly-α	24	2.813	0
0537–286	2.974	20.3	U	Ly-α	20	3.104	29
0906+430[c]	0.63	–	U	Ly-α	25	0.670	69
0957+561A	1.391	20.3	U	Ly-α	26	1.413	17
1225+317	1.7941[d]	19.4	U	Ly-α	27	2.219	173
1354–107	2.996	20.8	U	Ly-α	20	3.006	2
1354+258	1.4205	21.5	U	Mg II	28	2.006	326
1451–375	0.2761	20.1	U	Ly-α	29	0.314	100
2128–123	0.4298	19.4	U	Mg II	30	0.501	150
2223–052[e]	0.4842	20.9	U	Ly-α	31	1.4040	941
2342+342	2.9084	21.3	U	Ly-α	18	3.053	34

Notes: [†]Just prior to this paper being accepted, a detection of 21-cm absorption in this DLA was published (Kanekar et al. 2006). This was previously flagged a non-detection by Curran et al. (2005), although the data and subsequent limit were poor. [a]3C196, [b]3C286, [c]3C216, [d]21-cm absorption searched at $z = 1.795$, although the 5 MHz bandwidth used should cover $1.781 \lesssim z_{\rm abs} \lesssim 1.808$ (Briggs & Wolfe 1983), [e]3C446.

References: [1]Burbidge et al. (1976), [2]Steidel & Sargent (1992), [3]Wolfe et al. (1985), [4]Boulade et al. (1987), [5]Rao & Turnshek (1998), [6]Brown & Mitchell (1983), [7]Ulrich & Owen (1977), [8]Bergeron & Boissé (1991), [9]Wright et al. (1979), [10]Kinman & Burbidge (1967), [11]Wright et al. (1979), [12]Wilkes et al. (1983), [13]Brown & Roberts (1973), [14]Young, Sargent & Boksenberg (1982), [15]Aldcroft, Bechtold & Elvis (1994), [16]Darling et al. (2004), [17]Falomo (1991), [18]White, Kinney & Becker (1993), [19]Gaskell (1982), [20]Ellison et al. (2001), [21]Wolfe et al. (1995), [22]Petitjean et al. (1996), [23]Burbidge et al. (1977), [24]Smith, Margon & Jura (1979), [25]Wills et al. (1995), [26]Wills & Wills (1980), [27]Ulrich (1976), [28]Barthel, Tytler & Thomson (1990), [29]Lanzetta, Wolfe & Turnshek (1995), [30]Weymann et al. (1979), [31]Le Brun et al. (1993).

size with redshift. It is also close to the redshift where the Lyman-α transition can be observed by ground based telescopes, thus giving the appearance that Lyman-α selected DLAs are less likely to be detected, although, as we see from Fig. 3, this is purely a consequence of the higher redshifts probed by this transition.

Using this partitioning, at $z_{\rm abs} < 1.6$, for ratios of $DA_{\rm DLA}/DA_{\rm QSO} < 0.8$, 21-cm absorption tends to be detected (11 out of 13 cases) and for $DA_{\rm DLA}/DA_{\rm QSO} > 0.8$, 21-cm absorption tends to be undetected (8 out of 10 cases). Within each range, if there is an equal likelihood of obtaining either a 21-cm
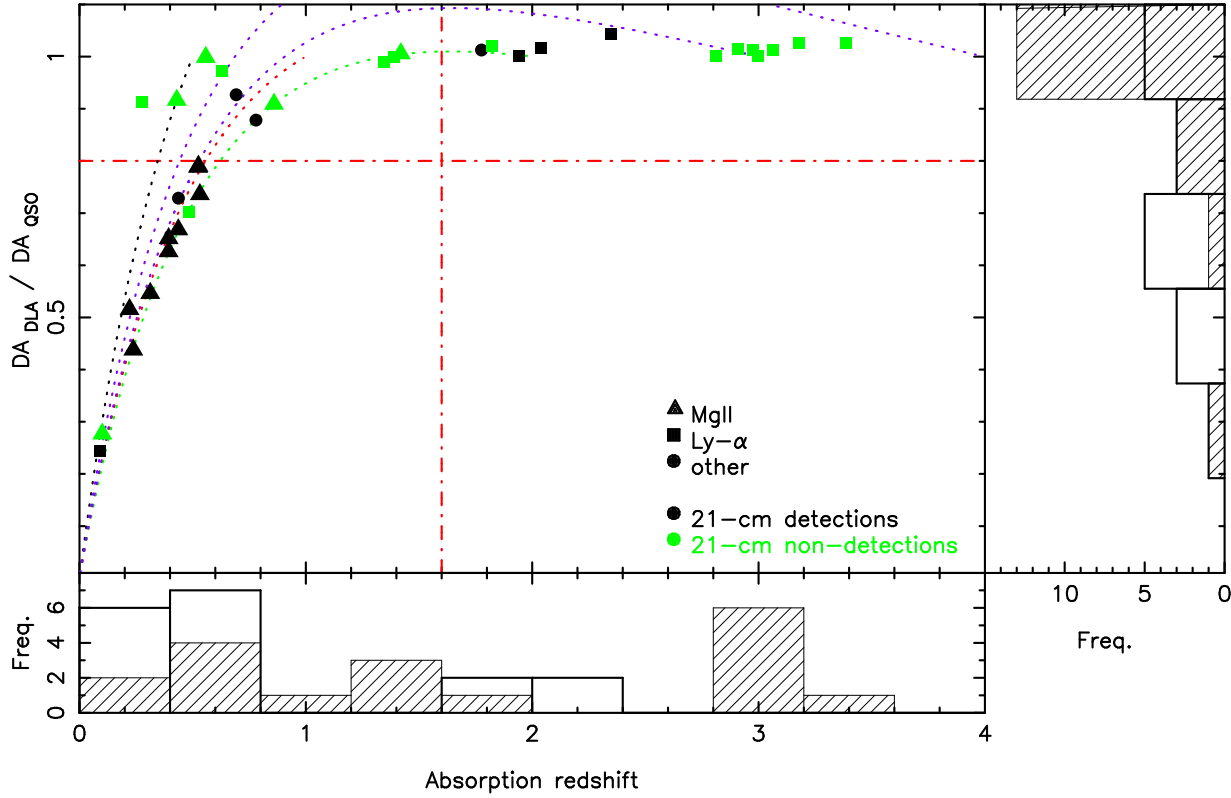
Figure 3. The absorber/quasar angular diameter distance ratio versus the absorption redshift. The black symbols represent the 21-cm detections and the coloured symbols the non-detections, with the shapes designating the transition through which the DLA was discovered. Note that 0235+164 and 0827+243 are coincident at $z_{\rm abs} \approx 0.52$ and $DA_{\rm DLA}/DA_{\rm QSO} \approx 0.79$. The iso-redshift curves show how $DA_{\rm DLA}/DA_{\rm QSO}$ varies with absorber redshift, where $DA_{\rm QSO}$ is for a given QSO redshift, given by the terminating value of $z_{\rm abs}$. That is, we show $DA_{\rm DLA}/DA_{\rm QSO}$ for $z_{\rm em} = 0.5, 1, 2, 3$ and 4.

detection or non-detection, the binomial probability of 11 or more out of 13 detections occurring in one bin, while 8 or more out of 12 non-detections occur in the other bin is just 0.06%. Changing the redshift partition to $z_{\rm abs} = 1$ gives a binomial probability of 0.25% and no redshift partition, i.e. $\geqslant 11/13$ detections in one bin with $\geqslant 16/22$ non-detections in the other bin, gives 0.03%. This leads to the hypothesis that high redshift ($z_{\rm abs} \gtrsim 2$) DLAs tend not to be detected in 21-cm absorption because $DA_{\rm DLA}/DA_{\rm QSO} \approx 1$ for all of these systems.

Fig. 3 illustrates that a redshift–distance ratio bias arises, since at $z_{\rm abs} \gtrsim 1.6$ the covering factor[5] becomes effectively independent of distance and is thereby determined by the relative extents of the absorption cross section and continuum emission region only. At lower redshifts (particularly $z_{\rm abs} \lesssim 1$) the close-to-linear decrease of angular size with distance means that, for a given absorption cross section, low redshift systems can much more effectively cover the background emission. That is, above $z_{\rm abs} \approx 1$, 21-cm absorption searches are disadvantaged by the fact that in all cases $DA_{\rm DLA}/DA_{\rm QSO} \approx 1$. Furthermore, the angular diameter–redshift relationship dictates that the bottom right-hand quadrant of Fig. 3 is destined to always remain empty and the higher the value of $z_{\rm em}$, the lower $z_{\rm abs}$ must be in order to yield $DA_{\rm DLA}/DA_{\rm QSO} < 1$.

Using the luminosity distances, a similar distribution to Fig. 3 is seen, with the concentration of 21-cm detections occurring at

$D_{\rm DLA}/D_{\rm QSO} < 0.5$ and the majority of non-detections having luminosity distance ratios of $D_{\rm DLA}/D_{\rm QSO} > 0.8$. Therefore, as well as affecting the effective coverage of the quasar's emission, the generally close DLA–QSO proximity in the high redshift sample (Fig. 2) could have implications for the spin temperature of the 21-cm absorbing gas in the DLA through increased incident 21-cm flux. We now investigate this possibility as well as attempting to quantify the effect of the proximity bias on the covering factors.

2.2 Spin temperatures

The high incidence of H I 21-cm non-detections with large fractional distances raises an interesting possibility: In order to explain the decrease in the number density of Lyman-α absorbers as $z_{\rm abs} \rightarrow z_{\rm em}$, against the general increase in the number density with redshift, Weymann, Carswell & Smith (1981); Bajtlik, Duncan & Ostriker (1988) invoke a "proximity effect", where at close to $z_{\rm em}$ the absorber is subject to a high ionising flux from the quasar it occults, thus reducing the number of Lyman-α clouds observed[6]. In light of the large number of 21-cm non-detections located relatively close to the background radio source, an analogy of the proximity effect may be at play, where a high 21-cm flux is maintaining a higher population in the upper hyperfine level (Wolfe & Burbidge 1975). This would decrease the observed

---

[5] As defined by $f \equiv \left(\frac{r}{r_{\rm QSO}}\right)^2 \cdot \left(\frac{DA_{\rm QSO}}{DA_{\rm DLA}}\right)^2$, see Equation 4.

[6] Note that there is also a galaxy proximity effect, where the gaseous envelopes of galaxies close to QSOs are rarer and smaller than their QSO remote counterparts (Pascarelle et al. 2001).
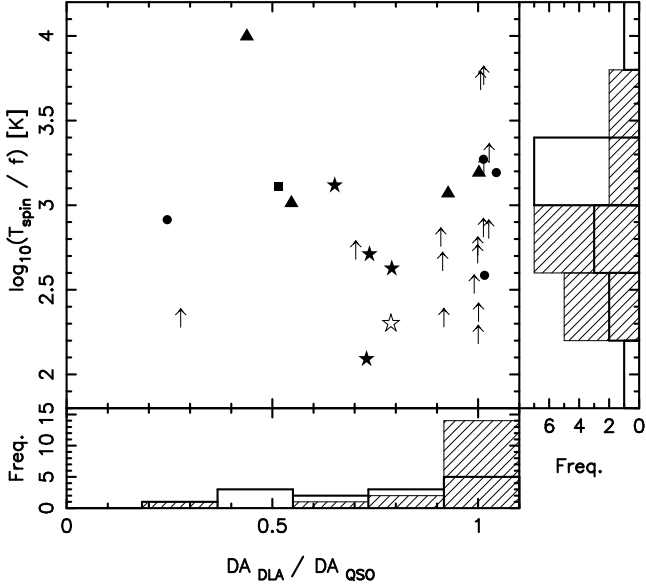
Figure 2. Spin temperature/covering factor ratio versus the absorber/quasar angular diameter distance ratio. The symbols represent the 21-cm detections and the shapes represent the type of galaxy with which the DLA is associated: circle–unknown type, star–spiral, square–dwarf, triangle–LSB. The arrows show the lower limits and all of these bar one (0454+039 at $z_{abs} = 0.8596$) have unknown host identifications (Table 1). The unfilled star represents 0235+164 (a spiral at $z_{abs} = 0.524$): The 21-cm absorption in this DLA is optically thick (Roberts et al. 1976) and so we assume $f = 1$ which, when combined with $N_{HI} \approx 5 \times 10^{21}$ cm^{-2} (Junkkarinen et al. 2004), gives $T_{spin} \approx 200$ K. Throughout this paper the bold histogram represents the 21-cm detections and the hatched histogram the upper limits/non-detections.

H I 21-cm optical depth through an increase in stimulated emission (Equation 1).

The intrinsic luminosity of the quasar at the rest frame emission frequency, ν_{em}, is $L_\nu = 4\pi D_{QSO}^2 S_{obs}/(z_{em} + 1)$, where D_{QSO} is the luminosity distance to the quasar, S_{obs} is the observed flux density (given in Table 1 of Curran et al. 2005) and $z_{em}+1$ is the k-correction (Bajtlik, Duncan & Ostriker 1988; Hogg 1999). Furthermore, the 1420 MHz flux density at the absorber is $S_{1420} = L_\nu/4\pi \Delta D^2$, where ΔD is the luminosity distance between the absorber and the quasar. Combining this with the previous equation gives

$$S_{1420} = \frac{S_{obs}}{(z_{em} + 1)} \frac{D_{QSO}^2}{\Delta D^2} \, . \tag{2}$$

Since the observed frequency is given by both $\nu_{obs} = \nu_{abs}/(z_{abs} + 1)$ and $\nu_{obs} = \nu_{em}/(z_{em} + 1)$, the continuum emission frequency in the rest frame of the quasar is given by $\nu_{em} = \nu_{abs}(z_{em} + 1)/(z_{abs} + 1)$ [where $\nu_{abs} = 1420$ MHz in the rest frame of the absorber]. From this, the redshift of the quasar in the rest frame of the absorber is given by

$$\Delta z = \frac{z_{em} + 1}{z_{abs} + 1} - 1, \tag{3}$$

which we use to determine ΔD.

In Fig. 4 we show the observational results of the H I 21-cm searches (the spin temperature/covering factor ratio) against the 21-cm flux density calculated at a distance ΔD from the quasar. From this we see that below a flux density of $\sim 10^4$ Jy at the absorber, there is no overwhelming difference in the 21-cm detections and
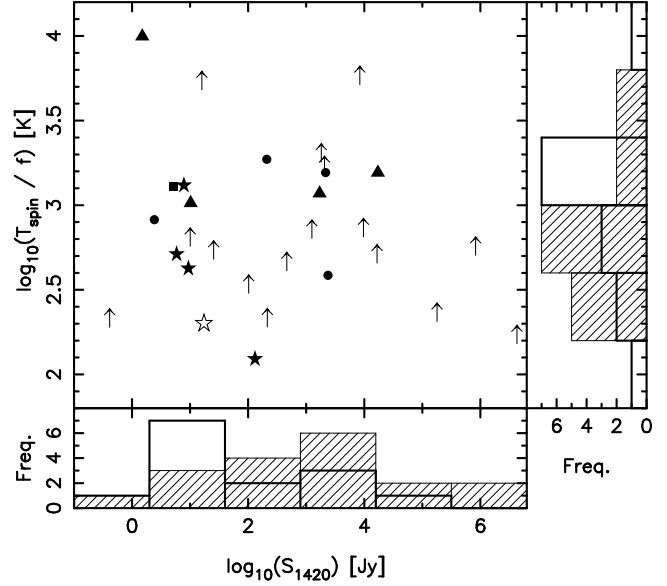

Figure 4. Spin temperature/covering factor ratio versus the 21-cm flux density at the absorber. The symbols are as per Fig. 2.

non-detections, although the latter do tend to be more slightly numerous above ~ 100 Jy, as well as being dominant at $\gtrsim 10^4$ Jy. However, the numbers are small and it appears as though increased flux densities due to close proximity to the background source is not the dominant cause of the non-detection of 21-cm absorption.

2.3 Covering factors

Since it appears that the non-detections are not due to spin temperatures being raised by the quasar flux, we now focus on the how the covering factor varies with quasar proximity. As usual, we cannot separate out the relative contributions from the spin temperature and the covering factor, although we can define, using the small angle approximation[7], the covering factor as

$$f \equiv \frac{r^2}{DA_{DLA}^2.\theta_{QSO}^2}, \tag{4}$$

where r is the 21-cm absorbing cross section and θ_{QSO} is the radio source size as determined from high resolution observations (see Table 2 of Curran et al. 2005). It should be borne in mind that these are usually measured at frequencies which are several times higher than the redshifted 21-cm (1420 MHz) line. In addition to assuming that these provide an accurate indicator of the radio source size at the absorption frequency, Equation 4 also assumes that the emission is uniform over the extent of this radio emission.

If these assumptions are reasonable, substituting Equation 4 into Equation 1 allows us to plot a covering factor "free" version of Fig. 2, which we show in Fig 5. In the plot, like figures 4 and 5 of Curran et al. (2005), we see a clear distinction between the distribution of the spirals and the more compact galaxies (more evident in Fig. 6). This may indicate that, at least at low redshift (where $D_{DLA}/D_{QSO} < 0.8$), each group has similar ratios ($T_{spin}/r^2 \sim 10^6$ K kpc^{-2} for the compact galaxies and ~ 0.1 K kpc^{-2} for the spirals), with the absorbing cloud size making a large

---

[7] Which applies to all of the background radio sources here since $\theta_{QSO} \leqslant 64''$.
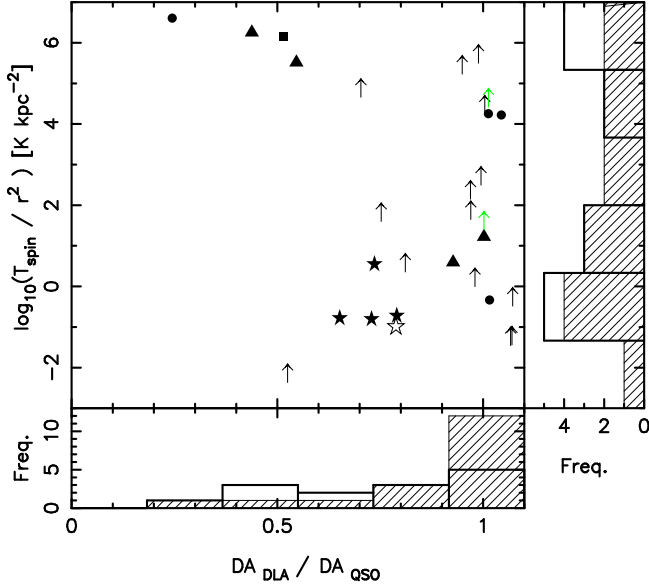
Figure 5. Spin temperature/absorbing radius ratio versus the absorber/quasar angular diameter distance ratio. The symbols are as per Fig. 2, with the coloured arrows designating the lower limits due to upper limits in the radio source sizes for the detections ($< 1.2''$ and $< 0.04''$, Table 2 of Curran et al. 2005). Note the there are also four such cases in the 21-cm non-detections (0201+113, 0335–122, 0454+039 & 1225+317), but since we do not discuss these they are shown at their current lower limits.

contribution in the very different values between these two groups: A span of ≈ 7 orders of magnitude seems unlikely through spin temperature alone, although for a given temperature, a span of only ~ 3 dex is required in the radius of the absorbing region. Furthermore, figure 4 of Curran et al. (2005) shows that the radio sources of $\lesssim 0.1''$ tend to be adequately covered by the compact galaxies, whereas for the larger radio sources spirals are required.

Bearing in mind that two of the $T_{\rm spin}/r^2$ values at $DA_{\rm DLA}/DA_{\rm QSO} \approx 1$ ($D_{\rm DLA}/D_{\rm QSO} \gtrsim 0.8$) are lower limits, in Fig. 5 there may be a trend for $T_{\rm spin}/r$ to decrease as the DLA–QSO distance (angular diameter & luminosity) closes, for 21-cm absorption detected in non-spirals. Presuming that the spin temperature does not decrease with proximity to the quasar (contrary to what we would expect)[8], this may suggest a selection effect where only large 21-cm absorbers are detected close to the background continuum, implying that self shielding against high fluxes are important, where the effectiveness of this scales with cloud size (Fig. 6). This, however, relies upon the aforementioned assumptions regarding the radio sources and many more detections would be required to adequately test this hypothesis. We note with interest, that the 21-cm detection located furthest to the bottom right in Fig. 5 (absorber ID unknown at $DA_{\rm DLA}/DA_{\rm QSO} = 1.02$), which has the very low value of $T_{\rm spin}/r^2 = 0.46$ K kpc^{-2} ($r/\sqrt{T_{\rm spin}} = 1.5$ kpc K$^{-1/2}$, Fig. 6), is due to 0458–020, where a large absorbing cross section of $r > 10$ kpc is deduced from VLA and VLBI observations (Briggs et al. 1989).
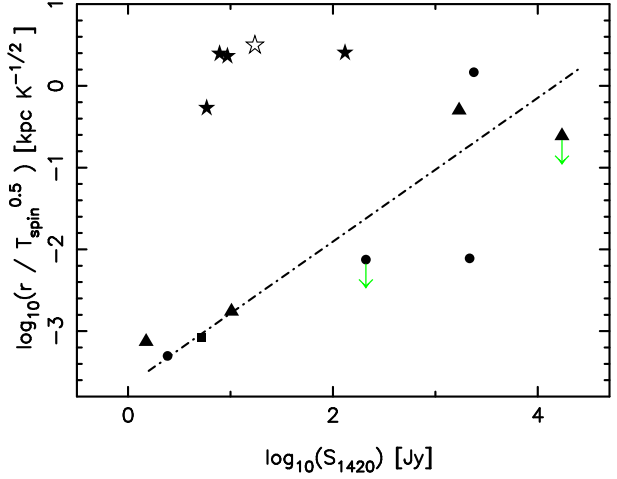

Figure 6. The 21-cm absorbing cross section/spin temperature versus the 21-cm flux density at the absorber for the 21-cm detections. The symbols are as per Fig. 5 and the fit is for the seven non-spirals without upper limits and is characterised by a gradient of 0.88 and an intercept of -3.66 (the regression coefficient is 0.86).

3   SUMMARY

Regarding the detectability of 21-cm absorption in DLAs, we have found:

• In general, the non-detections of 21-cm absorption in DLAs have been searched as deeply as the detections, meaning that the ratio of spin temperature/covering factor does not differ significantly between the two samples.

• There is an apparent bias for 21-cm absorption to be detected in DLAs originally discovered through the Mg II doublet rather than the Lyman-α line. This, however, is superficial and merely reflects the true bias introduced by the redshift distribution of the DLAs:

At $z_{\rm abs} \gtrsim 1.6$, the absorbers are effectively at the same (angular) distances as the background quasars. After ruling out the possibility that the closer proximity of the undetected DLAs to the background quasars significantly raises the spin temperatures above those of the detections, we believe that the non-detections are due to low covering factors, the result of the flattening of the angular diameter distance at $z \gtrsim 1$.

Since DLAs are not detected in 21-cm absorption at $z_{\rm abs} \geqslant 2.04$[9], Chengalur & Kanekar (2000); Kanekar & Chengalur (2001, 2003) suggested that the non-detections are due to the high redshift ($z_{\rm abs} \gtrsim 2$) DLAs having exclusively high spin temperatures and the presence of both 21-cm detections and non-detections at low redshift is attributed to a mix of spin temperatures. However, the distribution of 21-cm detections and non-detections closely follows that of low and high angular diameter distance ratios, respectively, so that high redshift DLAs have exclusively high ratios, whereas $z_{\rm abs} \lesssim 2$ systems exhibit a mix of ratios. This geometric effect means that absorbers at high redshift will always cover the background quasar much less effectively than at low redshift and the degeneracy between spin temperature and covering factor may only ever be resolved by targeted searches for 21-cm absorption in high redshift DLAs towards very compact radio sources.

---

[8] This suggests that the spin temperature also decreases with redshift, contrary to the results of Kanekar & Chengalur (2003).

[9] The highest redshift of a confirmed detection is now $z_{\rm abs} = 2.347$ (Table 1).

REFERENCES

Aldcroft T. L., Bechtold J., Elvis M., 1994, ApJS, 93, 1

Bajtlik S., Duncan R. C., Ostriker J. P., 1988, ApJ, 327, 570

Barthel P. D., Tytler D. R., Thomson B., 1990, A&AS, 82, 339

Bergeron J., Boissé P., 1991, A&A, 243, 344

Boulade O., Kunth D., Tytler D., Vigroux L., 1987, in et al. J., ed., High Redshift and Primeval Galaxies, Gif-sur-Yvette: Editions Frontiéres, pp 349–353

Briggs F. H., Wolfe A. M., 1983, ApJ, 268, 76

Briggs F. H., Wolfe A. M., Liszt H. S., Davis M. M., Turner K. L., 1989, ApJ, 341, 650

Brown R. L., Mitchell K. J., 1983, ApJ, 264, 87

Brown R. L., Roberts M. S., 1973, ApJ, 184, L7

Burbidge E. M., Caldwell R. D., Smith H. E., Liebert J., Spinrad H., 1976, ApJ, 205, L117

Burbidge E. M., Smith H. E., Weymann R. J., Williams R. E., 1977, ApJ, 218, 1

Chengalur J. N., Kanekar N., 2000, MNRAS, 318, 303

Churchill C. W., Kacprzak G. G., Steidel C. C., 2005, in Williams P., Shu C.-G., Menard B., eds, IAU Colloq. 199: Probing Galaxies through Quasar Absorption Lines, pp 24–41

Curran S. J., Murphy M. T., Pihlström Y. M., Webb J. K., Purcell C. R., 2005, MNRAS, 356, 1509

Curran S. J., Webb J. K., Murphy M. T., 2006, MNRAS, In preparation

Darling J., Giovanelli R., Haynes M. P., Bower G. C., Bolatto A. D., 2004, ApJ, 613, L101

Ellison S. L., et al., 2001, A&A, 379, 393

Falomo R., 1991, AJ, 102, 1991

Gaskell C. M., 1982, ApJ, 252, 447

Hogg D. W., 1999

Junkkarinen V. T., et al., 2004, ApJ, 614, 658

Kanekar N., Chengalur J. N., 2001, A&A, 369, 42

Kanekar N., Chengalur J. N., 2003, A&A, 399, 857

Kanekar N., Subrahmanyan R., Ellison S. L., Lane W. Chengalur J. N., 2006, MNRAS, Accepted (astro-ph/0605346)

Kinman T. D., Burbidge E. M., 1967, ApJ, 148, L59

Lanzetta K. M., Wolfe A. M., Turnshek D. A., 1995, ApJ, 440, 435

Le Brun V., Bergeron J., Boissé P., Christian C., 1993, A&A, 279, 33

Pascarelle S. M., Lanzetta K. M., Chen H.-W., Webb J. K., 2001, ApJ, 560, 101

Peacock J. A., 1999, Cosmological Physics. Cambridge University Press, Cambridge

Petitjean P., Théodore B., Smette A., Lespine Y., 1996, A&A, 313, L25

Prochaska J. X., Herbert-Fort S., Wolfe A. M., 2005, ApJ, 635, 123

Rao S. M., Turnshek D. A., 1998, ApJ, 500, L115

Roberts M. S., et al., 1976, AJ, 81, 293

Ryan-Weber E. V., Webster R. L., Staveley-Smith L., 2003, MNRAS, 343, 1195

Smith H. E., Margon B., Jura M., 1979, ApJ, 228, 369

Steidel C. C., Sargent W. L. W., 1992, ApJS, 80, 1

Stocke J. T., Foltz C. B., Weymann R. J., Christiansen W. A., 1984, ApJ, 280, 476

Ulrich M.-H., 1976, ApJ, 207, L73

Ulrich M.-H., Owen F. N., 1977, Nat, 269, 673

van Breugel W. J. M., et al., 1992, A&A, 256, 56

Weymann R. J., Carswell R. F., Smith M. G., 1981, ARA&A, 19, 41

Weymann R. J., Williams R. E., Peterson B. M., Turnshek D. A., 1979, ApJ, 234, 33

White R. L., Kinney A. L., Becker R. H., 1993, ApJ, 407, 456

Wilkes B. J., Wright A. E., Jauncey D. L., Peterson B. A., 1983, PASA, 5, 2

Wills B. J., et al., 1995, ApJ, 447, 139

Wills B. J., Wills D., 1980, ApJ, 238, 1

Wolfe A. M., et al., 1985, ApJ, 294, L67

Wolfe A. M., Burbidge G. R., 1975, ApJ, 200, 548

Wolfe A. M., Lanzetta K. M., Foltz C. B., Chaffee F. H., 1995, ApJ, 454, 698

Wright A. E., Morton D. C., Peterson B. A., Jauncey D. L., 1979, MNRAS, 189, 611

Wright A. E., Peterson B. A., Jauncey D. L., Condon J. J., 1979, ApJ, 229, 73

Young P., Sargent W. L. W., Boksenberg A., 1982, ApJS, 48, 455

Zwaan M. A., van der Hulst J. M., Briggs F. H., Verheijen M. A. W., Ryan-Weber E. V., 2005, MNRAS, 364, 1467